The Structural Era of Endocytosis

M. Marsh[1] and H. T. McMahon[2]

Endocytosis is crucial for an array of cellular functions and can occur through several distinct mechanisms with the capacity to internalize anything from small molecules to entire cells. The clathrin-mediated endocytic pathway has recently received considerable attention because of (i) the identification of an array of molecules that orchestrate the assembly of clathrin-coated vesicles and the selection of the vesicle cargo and (ii) the resolution of structures for a number of these proteins. Together, these data provide an initial three-dimensional framework for understanding the clathrin endocytic machinery.

The uptake, or endocytosis, of extracellular material into cells in membrane-bound vesicles has enthralled cell biologists for most of this century. The many functions in which endocytosis plays a role, including antigen presentation, nutrient acquisition, clearance of apoptotic cells, pathogen entry, receptor regulation, hypertension, and synaptic transmission, has stimulated this interest. But, there has also been a fascination with understanding the basic mechanisms that underlie endocytosis: for example, how plasma membrane is induced to form vesicles, how cell surface components are selectively included into these vesicles, and how the vesicle membrane and content are delivered to intracellular compartments. Endocytosis can occur through several morphologically and biochemically distinct mechanisms. Here, we focus on developments in the clathrin-mediated endocytic pathway.

The Clathrin Coat

Morphologically visible coats are seen on many vesicles that mediate transport between membrane-bound compartments in the cell. Coats function to deform the donor membrane to produce a vesicle, and they also function in the selection of the vesicle cargo. Three coat complexes have been well characterized so far: coat protein–I (COP-I), COP-II, and clathrin (*1*). COP-I coats are associated with vesicles that operate between the Golgi apparatus and the endoplasmic reticulum (ER) and at other steps within the Golgi and endosomal systems; COP-II coats are involved in transport from the ER to the Golgi. Clathrin coats are involved in two crucial transport steps: (i) receptor-mediated and fluid-phase endocytosis from the plasma membrane to early endosomes and (ii) transport from the trans-Golgi network (TGN) to endosomes. They may also function in transport from endosomes, immature secretory granules, and possibly other sites in the cell (*2*).

In endocytosis, the clathrin coat is assembled on the cytoplasmic face of the plasma membrane, forming pits that invaginate to pinch off (scission) and become free clathrin-coated vesicles (CCVs) (Fig. 1A). In cultured cells, the assembly of a CCV takes ~1 min, and several hundred to a thousand or more can form every minute (*3*). In other situations, such as the synapse, the clathrin cycle can be much faster and is tightly regulated (*4*). Clathrin-coated pits and CCVs can be identified in thin-section electron microscopy (EM) by the characteristic bristle density seen on the cytosolic side of coated membranes (Fig. 1A). EM imaging of deep-etched surfaces show these coats to be highly ordered polygonal arrays (Fig. 1B) (*5*), an organization also seen for isolated CCVs and clathrin cages (Fig. 1C) (*6, 7*). Studies published 25

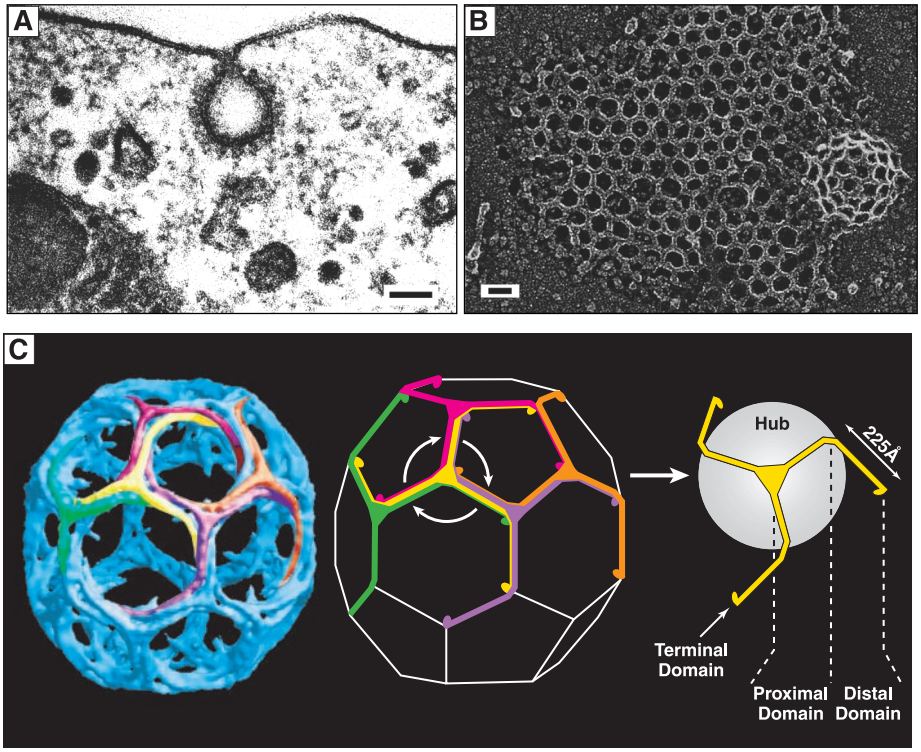

Fig. 1. Clathrin structures. (**A**) Thin-section EM illustrating the bristle coat associated with clathrin-coated pits and coated vesicles. Scale bar, 50 nm. (**B**) Deep-etch image of the cytosolic side of a plasma membrane showing the polygonal lattices of a coated pit and an invaginating coated vesicle. Reproduced from *The Journal of Cell Biology* (*57*) by copyright permission of the Rockefeller University Press. Scale bar, 33 nm. (**C**) A 21 Å resolution map of a clathrin hexagonal barrel assembled from purified clathrin and AP2 complexes (*7*). In vivo coated vesicles are larger; the minimum composition suggested to accommodate a vesicle is 60 triskelions assembled into 20 hexagons and 12 pentagons to achieve curvature. Each side of every polygon in the cage contains four segments of leg derived from four different triskelions. The proximal leg domains from adjacent hubs form an antiparallel pair on the top of each edge, and the distal domains make an antiparallel pair beneath. A small clockwise twist of the clathrin triskelion (as indicated with the yellow triskelion) would detach it from the cage. The middle and right panels show schematic views of the clathrin cage and the organization of the triskelion, respectively.

[1]Medical Research Council Laboratory for Molecular Cell Biology and Department of Biochemistry, University College London, Gower Street, London WC1E 6BT, UK. E-mail: m.marsh@ucl.ac.uk [2]Medical Research Council Laboratory of Molecular Biology, Hills Road, Cambridge CB2 2QH, UK. E-mail: hmm@mrc-lmb.cam.ac.uk

years ago gave the first indication of the composition of these coats (*8*). The main scaffold component is the 190-kD protein called clathrin heavy chain (CHC), which is associated with an ~25-kD protein called the clathrin light chain (CLC). These CHC-CLC complexes form three-legged trimers, called triskelions (Fig. 1C) (*9*), that can oligomerize both in vivo and in vitro to give the polygonal arrays seen with EM (*10*).

Other proteins found in the clathrin coat include the assembly protein AP180 and the adaptor complexes (APs). AP180 has clathrin assembly activity in vitro and is crucial for synaptic vesicle endocytosis and the maintenance of a uniform-sized vesicle population in vivo (*11*). APs can promote clathrin cage assembly, linking clathrin to the membrane and interacting with membrane proteins that contain appropriate signals for sorting into CCVs (*12*). Each AP contains four polypeptides, called adaptins: two of ~100 kD, a medium (μ) chain of ~50 kD, and a small (σ) chain of ~25 kD. These proteins form complexes that, by freeze-etch EM, appear as blocks from which the COOH-terminal domains of the two 100-kD adaptins protrude as appendages or ears (*13*). Different APs are associated with specific CCV populations and confer distinct sorting properties onto these vesicles. Thus, AP1 complexes are associated with CCVs derived from the TGN and contain γ, β1, μ1, and σ1 chains; AP2s are associated with endocytic CCVs and contain α, β2, μ2, and σ2 chains. Additional adaptor complexes, AP3 and AP4, have been identified but have not been characterized in detail (*14, 15*).

Another group of proteins that may also function as adaptors to link cell surface proteins to the clathrin scaffold are nonvisual arrestins (β-arrestin and arrestin-3) that mediate the internalization of activated heterotrimeric GTP–binding protein (G protein) coupled receptors (GPCRs) (*16*–*17*).

Clathrin

Pearse and colleagues used EM to generate the first detailed map of clathrin cages containing 8 hexagons and 12 pentagons (36 triskelions) (*6*). Low-temperature EM and developments in image analysis have allowed this structure to be resolved to 21 Å (Fig. 1C) (*7*). A triskelion hub domain is centered at each vertex of the cage, and three legs project in different directions from the hub (Fig. 1C). The legs are divided into a proximal and a distal domain by a bend midway along each. Thus, each leg contributes to two sides of a polygonal cell (Fig. 1C). The proximal leg domains form antiparallel pairs located on the outer surface of each edge. The distal leg domains lie along the underside of a second edge and position the NH_2-terminal domains of clathrin below the next hub, where they are oriented to interact with the APs located inside the cage. Thus, each edge is made up of four leg domains. The interlocking of the triskelions is such that a clockwise twist on any one could detach it from the cage (yellow triskelion in Fig. 1C). This may be the event catalyzed by heat shock cognate 70 (Hsc70) and auxilin, which disassembles the clathrin cage (*18*).

The crystal structure for the NH_2-terminal domain of the CHC was recently published (*19*). This 330–amino acid domain is a seven-bladed β propeller, similar to that found in, for example, the β subunits of heterotrimeric G proteins (Fig. 2). Prominent grooves are seen between blades 1 and 2 and blades 4 and 5 of the propeller. Residues Gln^{89}, Phe^{91}, Lys^{96}, and Lys^{98} lie on the margins of the groove between blades 1 and 2 and are crucial for arrestin binding (*17*). The clathrin-binding motif at the COOH-termini of nonvisual arrestins (*15, 17*) likely binds into this groove of the propeller. The clathrin-binding motif on AP2 has sequence similarity to that on the arrestins (*15*) and suggests that AP2 will also interact between blades 1 and 2 of this propeller.

A section of linker that couples the propeller to the distal leg was also seen in the terminal domain structure and is made up of a zigzag of 10 short α helices connected by loops (Fig. 2) (*19*). These helices pack onto each other in successive pairs to form a flexible stemlike structure. A similar structure was recently published for a fragment of the proximal leg of CHC that is involved in CHC polymerization and CLC association (*20*). This structure is an elongated right-handed superhelix that is also made up of short α helices linked by loops. However, in contrast to the flexibility in the linker region, the packing of the helices in the proximal leg fragment suggests a rigid structure.

Endocytosis Signals and Adaptors

Membrane proteins that are internalized in CCVs contain one or more signal sequences in their cytoplasmic domain or domains that direct the protein into clathrin-coated pits. Four types of endocytic sorting signals have

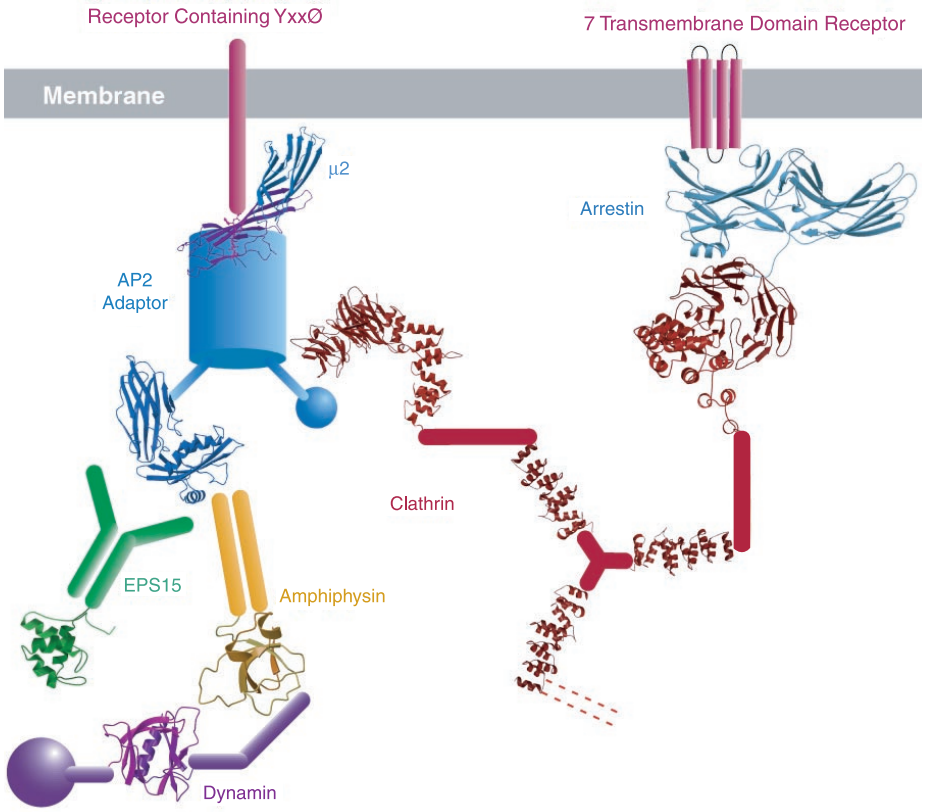

Fig. 2. Crystal and NMR structures of domains of proteins involved in clathrin-dependent endocytosis. The structures of COOH-terminal receptor-binding domain of AP2 μ2 (dark blue) [Protein Data Bank (PDB) identification (ID) code 1BXX], the ear domain of AP2 (dark blue) (PDB ID code 1b9k), the NH_2-terminal domain and linker of CHC (red) (PDB ID code 1BPO), a fragment of the proximal leg of the CHC (red) (PDB ID code 1b89) (only a section of the superhelix is shown), the SH3 domain of amphiphysin-2 (yellow) (PDB ID code 1BB9), the PH domain of dynamin (purple) (PDB ID codes 1dyn and 2dyn), the second EH domain of Eps15 (green) (PDB ID code 1EH2) are illustrated. These structures are not drawn to scale. The structure of visual arrestin (light blue) (PDB ID code 1AYR), which provides a model for interaction of the nonvisual arrestins (*58*) with CHC and might occupy a similar position to the AP2 complex, is also illustrated.

been identified (*12*): (i) tyrosine (Y)-based signals of the form FxNPxY (*21*) or YxxØ (where Ø is a large hydrophobic residue and x can be any amino acid, although Y+2 is frequently an R), (ii) dileucine (LL)-containing signals (*22*), (iii) a phosphorylated serine-rich domain at the COOH-terminus of many GPCRs (*16*), and (iv) motifs involving ligand-induced phosphorylation of serine residues and the ubiquitination machinery (*23*).

Both YxxØ and LL signals interact with AP2 complexes (*12*). For the YxxØ signals at least, this interaction is mediated by the AP2 μ2 chain. Co-crystallization of the signal-binding portion of μ2 with several YxxØ peptides has provided a structural explanation for this binding specificity (*24*). The μ2 fragment is an elongated banana-shaped β-sheet structure (Fig. 2). The YxxØ signal sequence binds to the surface of two parallel β strands of μ2 such that the side chains of the Y and Ø residues are oriented into two hydrophobic pockets in the surface of the μ subunit. The YxxØ peptides are bound in an extended conformation and not in the tight turn predicted by previous nuclear magnetic resonance (NMR) analyses of internalization signals in solution. The hydroxyl group of the Y contributes to a network of interactions with residues of μ2 that form the hydrophobic pocket, explaining why F does not efficiently substitute for Y in YxxØ signals (*25*). However, the NH_2-terminus of the glucose transporter Glut4 does contain an F that is essential for its endocytosis (*26*). A similar F is also found in the NH_2-terminus of the water channel, aquaporin-2. Both of these proteins are inserted into the plasma membrane transiently, following cell stimulation, and are then subjected to endocytosis. Because they need to reside in the plasma membrane for a finite length of time, the presence of F instead of Y in the endocytosis signal may result in weaker interactions with μ2 and slower endocytosis. The μ2 crystal structure also indicates that phospho-tyrosine would not bind into its hydrophobic pocket. Thus, the phosphorylation, and switching off, of some Y-based signals could provide an endocytic regulatory mechanism (*27*). The binding site on AP2 for LL signals is not yet clearly established (*28*); however, the YxxØ binding site on μ2 may only bind LL signals weakly, if at all.

It is unclear whether recruitment of AP2 complexes to the plasma membrane requires association with proteins (*29, 30*). Clathrin and APs alone can form cages on liposomes in vitro, indicating that a protein receptor may not be essential for pit formation and that cage assembly can be sufficient to drive membrane deformation (*30*). The putative membrane-facing surface of μ2 has a positively charged surface potential that could facilitate electrostatic binding of AP2 to the negatively charged membrane surface (*24*). Nevertheless, recruitment of coat components may be more efficient on cellular membrane preparations (*29, 30*), and membrane-associated proteins may still facilitate coat recruitment.

Various important residues used in the complex of μ2 with internalization signals are not conserved in other μ chains (for example, $Lys^{420} \rightarrow Pro^{420}$ in μ1 and $Lys^{203} \rightarrow Cys^{203}$ in μ3a). These variations likely account for subtle differences in the signal recognition properties of different adaptors, thus allowing selective cargo incorporation into vesicles derived from different membrane systems (*12*). The existence of consensus sequences for internalization allows one to begin to predict candidate proteins that could be internalized by endocytic CCVs. For example, many of the integral membrane proteins of synaptic vesicles have YxxØ sequences (for example, Scamp 37 and synaptophysin), although these sequences have not yet been shown to function as endocytosis signals in these proteins. The identification of μ-chain residues that are key to signal recognition has enabled the generation of dominant negative μ2 constructs, which will allow the probing of specific functions of AP2 complexes (*31*).

In addition to μ2, the crystal structure of a second element of the AP2 complex, the α-adaptin appendage (ear) domain has been solved (*32*). With the structural solution and dominant negative experiments based on the structure, the importance of this domain is beginning to be appreciated. The NH_2-terminal β-sandwich subdomain appears to function as a scaffold and spacer that support a COOH-terminal platform subdomain to which various proteins implicated in endocytosis (including the amphiphysin, Eps15, epsin, AP180, and auxilin) bind. The binding site is centered around Trp^{840} and is surrounded by

Table 1. Structures determined for proteins involved in clathrin-mediated endocytosis. 2D, two-dimensional.

Protein	Structural solution	Resolution (Å)	Critical interacting residues	Binding partners
Clathrin	EM, negative staining; clathrin trimers (*9*)	~25 (2D)	Gln^{89}, Phe^{91}, Lys^{96}, Lys^{98} for arrestins (*17*)	
	EM, rotary shadow and deep-etch; clathrin trimers (*5, 57*)	~25 (2D)		
	EM, negative staining; clathrin hexagonal barrels (*6*)	~25		
	Cryo EM; clathrin hexagonal barrels (*7*)	21		
	Crystallography; NH_2-terminal domain of clathrin heavy chain (CHC) residues 1 to 494 (*19*)	2.6		Adaptor proteins, arrestins, auxilin, amphiphysin, AP180
	Crystallography; CHC proximal leg domain residues 1210 to 1516 (*20*)	2.6		CHC proximal leg, clathrin LC
Adaptors	EM, rotary shadow and deep-etch; AP complexes (*13*)	~25 (2D)		
	Crystallography; AP2 μ2 residues 158 to 435 (*24*)	2.7	Phe^{174}, Arg^{423} (*24*)	YxxØ endocytosis signals
	Crystallography; AP2 COOH-terminal α-adaptin appendage domain residues 701 to 938 (*32*)	1.9	Trp^{840}, Glu^{907}, Arg^{920} (*32*)	AP180, amphiphysin, auxilin, Eps15, epsin
Eps15	EM, rotary shadow (*52*)	~25 (2D)	Trp^{169} (*55*)	Epsin, AP2, synaptojanin, AP180
	NMR; second EH domain residues 121 to 218 (*55*)			
Amphiphysin SH3 domain	Crystallography (*41*)	2.2	Glu^{39}, Asp^{60}, Trp^{63}, Phe^{89} (*41*)	Dynamin, synaptojanin
Dynamin PH domain	Crystallography (*48*), NMR (*47*)	2.2	Lys^{535} (*45*)	PIP_2
Visual arrestin	Crystallography (*58*)	3.3		Clathrin NH_2-terminal domain binds the COOH-terminal domain of nonvisual arrestins

mainly charged residues. It was observed that each of the appendage domain ligands have conserved DPF or DPW motifs (*21, 33, 34*), and these were shown to be involved in the interaction with the single binding pocket on the COOH-terminal subdomain (*32*). Thus, the ear domain recruits key components of the CCV assembly machinery in a spatially and temporally regulated fashion. The structure of the β2 ear has yet to be established, as do its binding partners [other than clathrin, which interacts with the β2 hinge region (*15*)].

The terminal domains from three separate triskelions sit under each vertex of the cage (Fig. 1C) and can be traced onto electron density seen in the 21 Å map (*35*). The terminal domains are positioned to interact with APs and electron density from the NH_2-terminus appears continuous with the APs in the 21 Å structure (*8*). If three terminal domains are found under each vertex, there could be three APs per vertex (that is, one adaptor per head domain). However, visualization of transferrin receptors located in coated pits suggest just one receptor per vertex and thus possibly only one AP2 complex (*36*).

Clathrin- and Adaptor-Associated Proteins

In addition to the basic scaffold proteins that form clathrin-coated structures, other proteins can bind to either clathrin or clathrin APs (Table 1 and Fig. 3). Most of these proteins do not copurify stoichiometrically with CCVs and are therefore thought to modulate cage assembly, vesicle scission, cage disassembly, or recycling of the structural components of the coat. These proteins interact using a variety of defined structural modules like the protein-lipid recognition module [pleckstrin homology (PH) domain] or various protein-protein recognition modules [for example, SRC homology 3 (SH3) domain, coiled-coil domain, proline-rich domain, and Eps15 homology (EH) domain] and are likely regulated by phosphorylation and dephosphorylation reactions (*37*). Moreover, the functional role of these proteins has, in many cases, been demonstrated through the ability of isolated domains to function as dominant negative inhibitors of receptor-mediated endocytosis.

Dynamin and Amphiphysin

The mechanism by which an invaginated coated pit is converted to a vesicle remains unclear. A cytoplasmic guanosine triphosphatase (GTPase), dynamin, is thought to be a key player in this step. *Drosophila* carrying the temperature sensitive *Shibire* mutation in dynamin and cells expressing GTPase-defective forms of dynamin exhibit endocytosis defects that correlate with a lack of vesicle scission (*38*). Moreover, dynamin has been located on the necks of deeply invaginated pits by EM (*38*).

The means by which dynamin is recruited to clathrin-coated pits have recently received particular attention. Amphiphysin, a cytosolic protein that can simultaneously bind the AP2 α ear and dynamin through different domains (*39*), has been implicated in dynamin recruitment. The SH3 domain of amphiphysin binds to a proline-rich domain in dynamin, and disruption of this interaction by peptides or recombinant amphiphysin SH3 domains blocks recruitment of dynamin to coated pits and clathrin-mediated endocytosis (*39, 40*). The amphiphysin SH3 domain not only binds dynamin but also prevents dynamin's assembly into oligomers. Crystallization shows that the amphiphysin-2 SH3 domain (Fig. 2) contains an enlarged n-Src loop that is at least partially responsible for the SH3 prevention of dynamin assembly (*41*). Because dynamin will polymerize at high concentrations, amphiphysin may ensure that dynamin is kept in a dissociated form at the sites of endocytosis until it is required for the scission reaction. In the nerve terminal, at least, the amphiphysin-dynamin interaction is also negatively regulated by phosphorylation of dynamin on serine residues (*37*). This modification may allow a primed endocytic machinery to be rapidly switched on by regulating the availability of dynamin for binding to the vesicle neck.

How does dynamin participate in the endocytosis event? Purified dynamin can constrict lipid vesicles to form long tubelike structures, with diameters similar to those found on the necks of forming endocytic vesicles (*30, 42*). These structures are seen in the absence of nucleotides and demonstrate that dynamin alone is capable of inducing tubule formation. Other factors may also contribute to vesicle neck formation, such as the closure of the clathrin cage, which results in a tight confinement of membrane through the lattice, or a specific lipid composition may favor the formation of this structure. Although dynamin may not be essential for the formation of deeply invaginated coated pits, it does seem to limit the neck diameter, as disruption of the dynamin-amphiphysin interaction in the lamprey synapse results in the accumulation of endocytosis profiles that are not tightly constricted (*40*). Dynamin's GTPase activity is not likely to be required for vesicle neck formation, but it's GTPase activity is required for endocytosis. The molecular details of the vesicle scission are yet unresolved, but three models have been put forward for dynamin's function in this step. One model proposes that scission occurs on constriction by dynamin of the vesicle's neck after GTP hydrolysis, causing the bilayers to fuse and the vesicle to be released (*42*). Another model shows that GTP hydrolysis can cause a concerted elongation of a dynamin spiral, and so vesicle fission would be achieved by stretching of the vesicle neck (*43*). Alternatively, there is evidence that the GTPase activity of dynamin may not itself induce scission; rather, the dynamin GTPase may act as a switch to regulate downstream effectors that mediate the scission step (*44*). Further work is required to distinguish these possibilities.

Dynamin's interaction with acidic phospholipids is pivotal to its ability to form

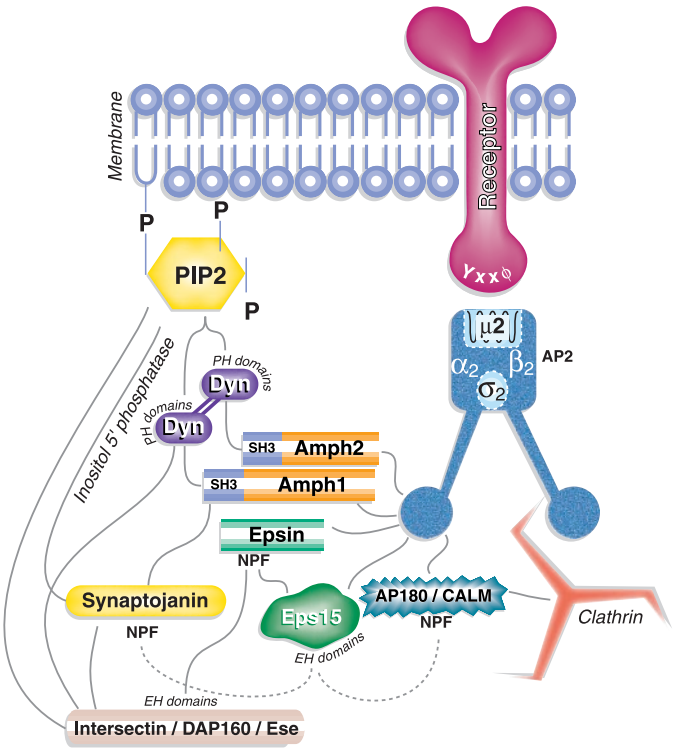

Fig. 3. Protein-protein interactions between clathrin and clathrin-associated proteins. The dashed lines indicate that the interactions between synaptojanin and Eps15 and between AP180 and Eps15 may not occur for neuronal forms of synaptojanin and AP180 that lack the NPF motifs. The interactions of multiple proteins with the α-adaptin ear domain are competitive, and thus, in vivo, there must be a sequential and spatial order to these interactions that are not represented in the diagram.

collars on invaginating vesicles and is mediated through its PH domain (*45*). This interaction is of low affinity, but binding may be enhanced by dimerization of the PH domains (*46*). The structure of the lipid-binding PH domain of dynamin has been solved (*47, 48*) (Fig. 2), and the selectivity of this domain for membranes containing phosphatidylinositol phosphate has been demonstrated biochemically (*48*). A preference for phosphatidylinositol-4,5-bisphosphate (PIP_2) may help to specify the region of the membrane in which dynamin oligomerization takes place. The cytosolic protein synaptojanin (which also binds to amphiphysin) is a phosphatidylinositol phosphatase (*49*), whose activity may be important in adjusting the inositol lipid composition of membranes and, thereby, regulating dynamin recruitment. However, this may not be the only function of this phosphatase, as the binding of AP180 and other APs to membranes also depends on phosphatidylinositol phosphates.

Dynamin's functions extend beyond CCV formation at the plasma membrane. There are at least three dynamin genes that together can generate 20 or more dynamin isoforms (*50*). Dynamin and dynamin-related proteins have been implicated not only in clathrin-dependent endocytosis but also in Golgi function, caveolae formation, and mitochondrial biogenesis (*50*). However, the observation that fluid-phase endocytosis is up-regulated in cells expressing a GTPase-defective dynamin that suppresses clathrin-mediated endocytosis indicates that cells may also use other endocytic pathways that employ distinct dynamin isoforms or alternative fission mechanisms (*51*).

Eps15 and EH Domains

Eps15 was initially identified as a major cytosolic substrate for ligand-activated epidermal growth factor (EGF) receptor tyrosine kinase. Interaction between Eps15 and the EGF receptor has not been detected, but Eps15 does bind AP2. Eps15 appears to have an extended conformation and forms linear oligomers (*52*). The amino acid sequence of Eps15 predicts that its central domain is likely to form a coiled coil. The NH_2-terminal domain has three repeats of an ~100–amino acid motif that has been termed the EH domain (*53*). EH domains are protein recognition modules that mostly bind sequences containing NPF (*21*), although some may recognize other motifs (*54*). The structure of an EH domain of Eps15 has been solved with NMR (*55*) (Fig. 2) and consists of a pair of EF hand motifs, one of which binds a calcium ion. The domain has a single NPF binding site. The calcium ion is likely to have a structural rather than a regulatory role, but a tryptophan residue located in a hydrophobic pocket is critical for binding NPF. Several NPF motif–containing proteins have been implicated in endocytosis, including Epsin, CALM, and nonneuronal isoforms of synaptojanin. Epsin (*33*) contains three NPF motifs in its COOH-terminal region and binds to Eps15. Epsin is homologous to intersectin binding protein 2 (IBP2), which also has three NPF motifs in its COOH-terminus. IBP2 binds to intersectin (a homolog of *Drosophila* DAP160 and the mammalian Ese proteins), which has two EH domains (*56*) and multiple SH3 domains, several of which bind to the proline-rich domains of dynamin and synaptojanin (Fig. 3).

Many protein-protein interactions are achieved with various combinations of interaction modules. Thus, SH3 domains interact with proline-rich domains in their binding partners, and side-chain variations of these domains give rise to specificity. EH domain–NPF interactions have low affinity, and residues around the NPF motif help to provide specificity (*54*). Many proteins contain multiple NPF repeats that could allow the binding of several EH domains and might increase binding affinity. However, the close proximity of some of these repeats would likely prevent multiple EH domain interactions.

The networks of contacts between clathrin-associated proteins, some of which are discussed above and others that are illustrated in Fig. 3, indicate the complexity of clathrin cage assembly. Not only are there a large number of proteins involved, but the connectivity of each of the proteins is achieved in multiple ways. Many of the interactions might appear redundant (for example, amphiphysin can associate directly with clathrin as well as through AP2). However, the various modes through which these interactions occur may coordinate and "fine-tune" the process of endocytosis, serving to efficiently recruit, in spatially and temporally distinct ways, the different proteins required at each stage of the cycle.

Conclusions

A high-resolution three-dimensional view of the clathrin coat is beginning to emerge. CCV formation is a complex process dependent on, and regulated by, the activities of a set of cytosolic proteins that are recruited through various protein-protein and protein-lipid interactions. Phosphorylation and dephosphorylation are emerging as key regulators of these interactions and of the activities of the proteins (*37*), but the precise order in which the different components act at each step of the process remains to be solved. Of all the coat-mediated transport events characterized so far, endocytic CCVs are unique in their amount of complexity. This may reflect a need for a higher degree of control to coordinate clathrin-mediated endocytosis in, for example, the rapid recovery of synaptic vesicle membrane or cellular responses to environmental stimuli. The developments seen over the past couple of years will continue; new insights and structures will be published soon. The challenge for the new century will be to understand how these structures interact to drive endocytosis.

References and Notes

1. M. S. Robinson, *Trends Cell Biol.* **7**, 99 (1997); B. S. Glick and V. Malhotra, *Cell* **95**, 883 (1998).
2. C. E. Futter *et al.*, *J. Cell Biol.* **141**, 611 (1998); W. Stoorvogel, V. Oorschot, H. J. Geuze, *ibid.* **132**, 21 (1996); L. Orci *et al.*, *Cell* **37**, 39 (1984); A. S. Dittie, N. Hajibagheri, S. A. Tooze, *J. Cell Biol.* **132**, 523 (1996).
3. M. Marsh and A. Helenius, *J. Mol. Biol.* **142**, 439 (1980); I. Gaidarov, F. Santini, R. Warren, J. H. Keen, *Nature Cell Biol.* **1**, 1 (1999).
4. P. De Camilli and K. Takei, *Neuron* **16**, 481 (1996); B. Marks and H. T. McMahon, *Curr. Biol.* **8**, 740 (1998).
5. J. Heuser, *J. Cell Biol.* **84**, 560 (1980).
6. G. P. Vigers, R. A. Crowther, B. M. Pearse, *EMBO J.* **5**, 529 (1986).
7. C. J. Smith, N. Grigorieff, B. M. Pearse, *ibid.* **17**, 4943 (1998).
8. B. M. Pearse, *Proc. Natl. Acad. Sci. U.S.A.* **73**, 1255 (1976).
9. T. Kirchhausen and S. C. Harrison, *Cell* **23**, 755 (1981); E. Ungewickell and D. Branton, *Nature* **289**, 420 (1981).
10. B. Pishvaee and G. S. Payne, *Cell* **95**, 443 (1998); E. Ungewickell, *Curr. Biol.* **9**, R32 (1999).
11. H. T. McMahon, *Curr. Biol.* **9**, R332 (1999).
12. T. Kirchhausen, J. S. Bonifacino, H. Riezman, *Curr. Opin. Cell Biol.* **9**, 488 (1997).
13. J. E. Heuser and J. Keen, *J. Cell Biol.* **107**, 877 (1988).
14. F. Simpson, A. A. Peden, L. Christopoulou, M. S. Robinson, *ibid.* **137**, 835 (1997); G. Shi, V. Faundez, J. Roos, E. C. Dell'Angelica, R. B. Kelly, *ibid.* **143**, 947 (1998); E. C. Dell'Angelica, C. Mullins, J. S. Bonifacino, *J. Biol. Chem.* **274**, 7278 (1999).
15. E. C. Dell'Angelica, J. Klumperman, W. Stoorvogel, J. S. Bonifacino, *Science* **280**, 431 (1998). A motif L(L or I)(D, E, or N)(L or F)(D or E) (*21*) in the β subunits of APs, the nonvisual arrestins, and amphiphysin (which also binds clathrin) is likely to account for the ability of these different proteins to bind clathrin.
16. S. S. Ferguson and M. G. Caron, *Semin. Cell Dev. Biol.* **9**, 119 (1998).
17. O. B. Goodman Jr., J. G. Krupnick, V. V. Gurevich, J. L. Benovic, J. H. Keen, *J. Biol. Chem.* **272**, 15017 (1997); J. G. Krupnick, O. B. Goodman Jr., J. H. Keen, J. L. Benovic, *ibid.*, p. 15011.
18. S. L. Schmid, W. A. Braell, D. M. Schlossman, J. E. Rothman, *Nature* **311**, 228 (1984); E. Ungewickell *et al.*, *ibid.* **378**, 632 (1995).
19. E. ter Haar, A. Musacchio, S. C. Harrison, T. Kirchhausen, *Cell* **95**, 563 (1998).
20. J. A. Ybe *et al.*, *Nature* **399**, 371 (1999).
21. Single-letter abbreviations for the amino acid residues are as follows: D, Asp; E, Glu; F, Phe; I, Ile; L, Leu; N, Asn; P, Pro; R, Arg; W, Trp; and Y, Tyr.
22. I. Sandoval and O. Bakke, *Trends Cell Biol.* **4**, 292 (1994).
23. L. Hicke, B. Zanolari, H. Riezman, *J. Cell Biol.* **141**, 349 (1998); R. Govers *et al.*, *EMBO J.* **18**, 28 (1999).
24. D. J. Owen and P. R. Evans, *Science* **282**, 1327 (1998).
25. I. S. Trowbridge, J. F. Collawn, C. R. Hopkins, *Annu. Rev. Cell Biol.* **9**, 129 (1993); M. M. Sauter *et al.*, *J. Cell Biol.* **132**, 795 (1996).
26. B. J. Marsh, R. A. Alm, S. R. McIntosh, D. E. James, *J. Cell Biol.* **130**, 1081 (1995).
27. T. Shiratori *et al.*, *Immunity* **6**, 583 (1997); D. J. Stephens and G. Banting, *FEBS Lett.* **416**, 27 (1997).
28. I. Rapoport, Y. C. Chen, P. Cupers, S. E. Shoelson, T. Kirchhausen, *EMBO J.* **17**, 2148 (1998); T. Bremnes, V. Lauvrak, B. Lindqvist, O. Bakke, *J. Biol. Chem.* **273**, 8638 (1998).
29. R. Le Borgne, G. Griffiths, B. Hoflack, *J. Biol. Chem.* **271**, 2162 (1996); Y. Zhu, L. M. Traub, S. Kornfeld, *Mol. Biol. Cell* **10**, 537 (1999).

30. K. Takei *et al.*, *Cell* **94**, 131 (1998).
31. A. Nesterov, R. E. Carter, T. Sorkina, G. N. Gill, A. Sorkin, *EMBO J.* **18,** 2489 (1999).
32. D. J. Owen *et al.*, *Cell* **97,** 805 (1999).
33. H. Chen *et al.*, *Nature* **394**, 793 (1998).
34. A. Benmerah, B. Begue, A. Dautry Varsat, N. Cerf Bensussan, *J. Biol. Chem.* **271**, 12111 (1996).
35. A. Musacchio *et al.*, *Mol. Cell* **3**, 761 (1999).
36. K. Miller, M. Shipman, I. S. Trowbridge, C. R. Hopkins, *Cell* **65**, 621 (1991).
37. V. I. Slepnev, G.-C. Ochoa, M. H. Butler, D. Grabs, P. De Camilli, *Science* **281**, 821 (1998).
38. S. L. Schmid, M. A. McNiven, P. De Camilli, *Curr. Opin. Cell Biol.* **10**, 504 (1998).
39. P. Wigge, Y. Vallis, H. T. McMahon, *Curr. Biol.* **7**, 554 (1997).
40. O. Shupliakov *et al.*, *Science* **276**, 259 (1997).
41. D. J. Owen *et al.*, *EMBO J.* **17**, 5273 (1998).
42. S. M. Sweitzer and J. E. Hinshaw, *Cell* **93**, 1021 (1998).
43. M. H. B. Stowell, B. Marks, P. Wigge, H. T. McMahon, *Nature Cell Biol.* **1**, 27 (1999).
44. S. Sever, A. B. Muhlberg, S. L. Schmid, *Nature* **398**, 481 (1999).
45. Y. Vallis, P. Wigge, B. Marks, P. R. Evans, H. T. McMahon, *Curr. Biol.* **9**, 257 (1999); A. Lee, D. W. Frank, M. S. Marks, M. A. Lemmon, *ibid.*, p. 261; M. Achiriloaie, B. Barylko, J. P. Albanesi, *Mol. Cell. Biol.* **19**, 1410 (1999).
46. D. E. Klein, A. Lee, D. W. Frank, M. S. Marks, M. A. Lemmon, *J. Biol. Chem.* **273**, 27725 (1998).
47. A. K. Downing *et al.*, *Curr. Biol.* **4**, 884 (1994); D. Timm *et al.*, *Nature Struct. Biol.* **1**, 782 (1994); D. Fushman, S. Cahill, M. A. Lemmon, J. Schlessinger, D. Cowburn, *Proc. Natl. Acad. Sci. U.S.A.* **92**, 816 (1995).
48. K. M. Ferguson, M. A. Lemmon, J. Schlessinger, P. B. Sigler, *Cell* **79**, 199 (1994); K. Salim *et al.*, *EMBO J.* **15**, 6241 (1996).
49. P. S. McPherson *et al.*, *Nature* **379**, 353 (1996).
50. H. Cao, F. Garcia, M. A. McNiven, *Mol. Biol. Cell* **9**, 2595 (1998); E. Smirnova, D. L. Shurland, S. N. Ryazantsev, A. M. van der Bliek, *J. Cell Biol.* **143**, 351 (1998); D. Otsuga *et al.*, *ibid.*, p. 333; R. Henley, E. W. Krueger, B. J. Oswald, M. A. McNiven, *ibid.* **141**, 85 (1998); S. F. Nothwehr, E. Conibear, T. H. Stevens, *ibid.* **129**, 35 (1995).
51. H. Damke, T. Baba, D. E. Warnock, S. L. Schmid, *J. Cell Biol.* **127**, 915 (1994).
52. P. Cupers, E. ter Haar, W. Boll, T. Kirchhausen, *J. Biol. Chem.* **272**, 33430 (1997).
53. F. Fazioli, L. Minichiello, B. Matoskova, W. T. Wong, P. P. Di Fiore, *Mol. Cell. Biol.* **13**, 5814 (1993); W. T. Wong *et al.*, *Proc. Natl. Acad. Sci. U.S.A.* **92**, 9530 (1995); P. P. Di Fiore, P. G. Pelicci, A. Sorkin, *Trends Biochem. Sci.* **22**, 411 (1997).
54. S. Paoluzi *et al.*, *EMBO J.* **17**, 6541 (1998).
55. T. de Beer, R. E. Carter, K. E. Lobel-Rice, A. Sorkin, M. Overduin, *Science* **281**, 1357 (1998).
56. J. Roos and R. B. Kelly, *J. Biol. Chem.* **273**, 19108 (1998); M. Yamabhai *et al.*, *ibid.*, p. 31401; A. S. Sengar, W. Wang, J. Bishay, S. Cohen, S. E. Egan, *EMBO J.* **18**, 1159 (1999). Endophilins also contain SH3 domains but lack EH domains [N. Ringstad, Y. Nemoto, P. De Camilli, *Proc. Natl. Acad. Sci. U.S.A.* **94**, 8569 (1997)].
57. J. E. Heuser, J. H. Keen, L. M. Amende, R. E. Lippoldt, K. Prasad, *J. Cell Biol.* **105**, 1999 (1987).
58. J. Granzin *et al.*, *Nature* **391**, 918 (1998); J. A. Hirsch, C. Schubert, V. V. Gurevich, P. B. Sigler, *Cell* **97**, 257 (1999).

59. We thank A. Pelchen-Matthews for Fig. 1A, J. Heuser for Fig. 1B, and B. Pearse and C. Smith for Fig. 1C; T. Kirchhausen, F. Brodsky, P. Hwang, and T. de Beer for providing structural coordinates; D. Owen and P. Evans for help in assembling Fig. 2; and A. Pelchen-Matthews, N. Signoret, M.-J. Bijlmakers, and P. Wigge for critical comments on the manuscript. We apologize to those whose work we have not cited because of limits on space. The authors are supported by the UK Medical Research Council.